Calhoun: The NPS Institutional Archive

Theses and Dissertations
Thesis Collection

1960-05-18

A spectrometer for study of neutron activation of beryllium-7 as a function of energy

Boyer, Walton T.

Monterey, California: U.S. Naval Postgraduate School

Calhoun is a project of the Dudley Knox Library at NPS, furthering the precepts and goals of open government and government transparency. All information contained herein has been approved for release by the NPS Public Affairs Officer.

Dudley Knox Library / Naval Postgraduate School
411 Dyer Road / 1 University Circle
Monterey, California USA 93943

http://www.nps.edu/library

NPS ARCHIVE
1960
BOYER, W.

A SPECTROMETER FOR STUDY OF NEUTRON ACTIVATION OF BERYLLIUM-7 AS A FUNCTION OF ENERGY

WALTON T. BOYER, JR.

$Be^7(n, \alpha)He^4$	$Q = 18.993$ Mev	$E_\alpha = 9.49$ Mev	$\sigma_{th} = 25$ mb
$Be^7(n, p)Li^7$	$Q = 1.646$ Mev	$E_\rho = 1.44$ Mev	$\sigma_{th} = 5.1 \pm 0.6 \times 10^5$ b.
$Be^7(n, p)Li^{7*}$	$Q = 1.168$ Mev	$E_\rho = 1.02$ Mev	

A search of the literature disclosed no other reported experiments on the effects of neutron interactions with Be^7. A comparison of the $Be^7(n, p)Li^7$ cross section reported by Hanna with the cross section of the mirror reaction $Li^7(p, n)Be^7$ indicates a discrepancy which can be explained by a resonance in Be^8 near the threshold level (Ha55, Ma58). Hanna's experiment exposed Be^7 to the full neutron spectrum of a thermal pile reactor, but did not determine the cross section as a function of incident neutron energy. It was felt that if a resonance does exist near threshold, it might very well be apparent in the $Be^7(n, p)Li^7$ cross section energy spectrum if the cross section were measured as a function of energy.

The purpose of the experiment described in this paper is to investigate the dependence of the $Be^7(n, p)Li^7$ cross section on the energy of the incident neutrons. The construction of a crystal neutron spectrometer at the Livermore Pool Type Reactor (LPTR) for the production of monoenergetic neutrons in thermal regions is described. Efforts at the development of a suitable detector for the reaction are continuing; results thus far obtained are subject to large contaminant errors. A description of the detectors used is included. Some preliminary results are discussed.

II. THE NEUTRON SPECTROMETER

A. General

Two types of neutron spectrometers were considered as methods for separating a monoenergetic beam of neutrons from the white radiation of the reactor. The first was a time-of-flight spectrometer, essentially a drum with helical grooves cut into its surface and revolving at high speeds. Operation of this instrument is based on limiting the upper and lower velocities of neutrons which may pass down the groove or channel without entering one or the other of the side walls. It is a natural extension of the neutron chopper. It was estimated that this instrument would

DUDLEY KNOX LIBRARY
NAVAL POSTGRADUATE SCHOOL
MONTEREY CA 93943-5101

UNIVERSITY OF CALIFORNIA
Lawrence Radiation Laboratory
Livermore, California

A SPECTROMETER FOR STUDY OF NEUTRON ACTIVATION OF BERYLLIUM-7 AS A FUNCTION OF ENERGY

Walton T. Boyer, Jr.

May 18, 1960

Submitted in partial fulfillment
of the requirements for the degree of
MASTER OF SCIENCE
IN
PHYSICS

United States Naval Postgraduate School
Monterey, California

NPS Archive
1960
Boyer, W.

~~THESIS~~

DUDLEY KNOX LIBRARY
NAVAL POSTGRADUATE SCHOOL
MONTEREY CA 93943-5101

A SPECTROMETER FOR STUDY OF NEUTRON ACTIVATION OF BERYLLIUM-7 AS A FUNCTION OF ENERGY

Walton T. Boyer, Jr.

Lawrence Radiation Laboratory, University of California
Livermore, California

May 18, 1960

ABSTRACT

A neutron diffraction crystal spectrometer with a resolution of 13 microseconds per meter and monochromatic beam intensity up to 10^4n/cm^2-sec in the range 0.012-0.400 ev has been constructed for study of the activation cross section of Be^7 as a function of energy in the thermal region. First preliminary results using ZnS(Ag) as a detector suggest the possibility of a resonance for the Be^7(n, p)Li^7 reaction in the region of 0.025-0.050 ev.

I. INTRODUCTION

This experiment developed out of a suggestion by Dr. Harold Brown inquiring into the neutron cross section of Be^7 as a function of energy. Two previous experiments have been conducted investigating the characteristics of Be^7 when exposed to thermal neutrons. The ground state of Be^7 was shown to have odd parity in an experiment by R. C. Hanna at Harwell, England (Ha 55). In that experiment, he observed a Be^7 reaction with a cross section of $5.3 \pm 0.8 \times 10^{-20} cm^2$* with a thermal pile spectrum of neutrons, and identified the events as resulting from $Be^7(n, p)Li^7$ interactions. From energy balance equations the $Be^7(n, \alpha)He^4$ interaction may be expected to predominate provided the parity of the compound nucleus is even. No such events were identified. Since appreciable cross sections for thermal neutrons are observed only for the incident neutron wave of zero angular momentum, the parity of the initial and compound nuclei are identical and the parity of ground state Be^7 was identified as odd.

In another experiment, R. E. Segel and others again attempted to identify $Be^7(n, \alpha)He^4$ events (Se 58). Again no events were identified as resulting from this interaction and a maximum thermal cross section of $2.5 \times 10^{-26} cm^2$ was established for the reaction.

Be^7 is a radioisotope with a half-life of 53.37 ± 0.11 days. It decays by K capture to Li^7. Of the decay events 11.5 ± 1% go by way of a 478-kev excited state of Li^7 with immediate γ transition to the ground state. The remainder of the decay events proceed directly to the ground state (Aj 59). The reactions that may be expected to occur upon thermal neutron bombardment of the Be^7 nucleus, the energy released from them, and the currently accepted cross sections are:

---

*The presently accepted value of $5.1 \pm 0.6 \times 10^{-20} cm^2$ apparently has come from this source; however, it is reported as $5.3 \pm 0.8 \times 10^{-20} cm^2$ in the original article.

$$\begin{array}{llll} Be^7(n,\alpha)He^4 & Q = 18.993\text{ Mev} & E_\alpha = 9.49\text{ Mev} & \sigma_{th} = 25\text{ mb} \end{array}$$

$$\left.\begin{array}{lll} Be^7(n,p)Li^7 & Q = 1.646\text{ Mev} & E_p = 1.44\text{ Mev} \\ Be^7(n,p)Li^{7*} & Q = 1.168\text{ Mev} & E_p = 1.02\text{ Mev} \end{array}\right\}\sigma_{th} = 5.1 \pm 0.6 \times 10^5\text{ b.}$$

A search of the literature disclosed no other reported experiments on the effects of neutron interactions with Be^7. A comparison of the $Be^7(n,p)Li^7$ cross section reported by Hanna with the cross section of the mirror reaction $Li^7(p,n)Be^7$ indicates a discrepancy which can be explained by a resonance in Be^8 near the threshold level (Ha55, Ma58). Hanna's experiment exposed Be^7 to the full neutron spectrum of a thermal pile reactor, but did not determine the cross section as a function of incident neutron energy. It was felt that if a resonance does exist near threshold, it might very well be apparent in the $Be^7(n,p)Li^7$ cross section energy spectrum if the cross section were measured as a function of energy.

The purpose of the experiment described in this paper is to investigate the dependence of the $Be^7(n,p)Li^7$ cross section on the energy of the incident neutrons. The construction of a crystal neutron spectrometer at the Livermore Pool Type Reactor (LPTR) for the production of monoenergetic neutrons in thermal regions is described. Efforts at the development of a suitable detector for the reaction are continuing; results thus far obtained are subject to large contaminant errors. A description of the detectors used is included. Some preliminary results are discussed.

II. THE NEUTRON SPECTROMETER

A. General

Two types of neutron spectrometers were considered as methods for separating a monoenergetic beam of neutrons from the white radiation of the reactor. The first was a time-of-flight spectrometer, essentially a drum with helical grooves cut into its surface and revolving at high speeds. Operation of this instrument is based on limiting the upper and lower velocities of neutrons which may pass down the groove or channel without entering one or the other of the side walls. It is a natural extension of the neutron chopper. It was estimated that this instrument would

provided a moneonergetic beam of neutrons up to about 1-ev peak energy, and with appropriate prior collimation of the beam, a resolution of about 40%. Such an instrument was under construction for Dr. A. Kirschbaum at this laboratory, but construction delays placed the availability of the instrument beyond the time limitations placed on this experimenter.

The second type of spectrometer considered was the neutron diffraction crystal spectrometer. Analogous in operation to the x-ray crystal spectrometer, the feasibility of operation of this type of instrument had been under consideration for many years. Its construction had to wait, however, until the development of the nuclear reactor, which made the production of high-flux thermal-neutron beams practical. The neutron diffraction crystal spectrometer has been used as a source of monoenergetic neutron beams for the study of crystalline structure, with particular emphasis on the magnetic characteristics of crystal structure, as is done at Harwell, England, and for the determination of total neutron cross section as a function of energy as is done at the Brookhaven National Laboratory. The crystal spectrometer is capable of high resolution and reliability in the low energy range. By proper selection of crystals, beams of monoenergetic neutrons from 0.01 ev to 50 ev may be produced. It has the drawback that the diffraction of the beam is based, as in the x-ray instrument, on Bragg diffraction phenomena; and therefore neutron contamination of higher order wavelengths will be present, in many instances in appreciable amounts.

A crystal spectrometer to provide a monochromatic beam of fixed wavelength for crystalline structure studies was under construction at the LPTR in the fall of 1959. Additional large single lead crystals from this experiment were made available to the author for use in a spectrometer in which the energy of the diffracted beam would be variable. Because of the opportunity thus presented, the crystal spectrometer was chosen as the source for a monoenergetic neutron beam and construction of a neutron diffraction crystal spectrometer was started.

B. Neutron Diffraction

Diffraction of the incident neutrons occurs, as in diffraction of x-rays, at certain well-defined energies. The mechanism of diffraction is based on the reinforcement of scattered wave amplitudes in certain directions by an orderly array of scattering centers. In the case of neutron diffraction, the scattering occurs at the atomic nuclei, and an orderly array of nuclei is provided conveniently in crystalline materials. When the array is such as to provide planes of atomic scattering centers for neutrons, the characteristic angle for reinforcement of the scattered neutron waves as measured from the atomic planes is given in the Bragg equation

$$n\lambda = 2d \sin \theta, \tag{1}$$

where n is the order of the reflection and takes on positive integer values, λ is the de Broglie wavelength of the scattered neutrons, d is the perpendicular interval between the scattering crystal planes, and θ is the angle between the scattering planes and the incident (or reflected) neutron path. The de Broglie wavelength of the neutron is defined by the relationship

$$\lambda = \frac{h}{\rho} = \frac{h}{(2mE)^{1/2}} \quad , \tag{2}$$

where h is Planck's constant, and ρ is the momentum of the neutron of energy E and mass m.

Higher order reflections are generally present and in thermal regions may be appreciable, but their intensity drops off very rapidly with the order of the reflection. The intensity of the diffracted radiation is dependent on a number of factors. For a large single crystal, they include coherent and incoherent elastic and inelastic scattering cross sections, thickness of the crystal, attenuation in the crystal, the mosaic spread in the crystal, and magnetic and thermal effects. Most large crystal are not true single crystals, but consist of many true single crystals of very small dimension, called mosaics, all oriented very nearly parallel to each other.

Using a prime to indicate terms referring to monoenergetic or monochromatic radiation, the intensity of a diffracted monochromatic beam may be expressed:

$$I_2' = I_1' R \, , \tag{3}$$

where I_1' is the intensity of the incident radiation of the proper energy for primary diffraction, I_2' is the intensity of diffracted beam, and R is the reflectivity of the crystal. Bacon (Ba 55b) expresses this in terms of the integrated reflection for a single crystal rotated in a beam of monochromatic radiation, R'. In this case

$$I_2' = I_1' R' \; 2d \cos \theta \, . \tag{4}$$

R' may be measured by recording the intensity of the diffracted beam as the crystal is rotated, using highly collimated incident and reflected beams and maintaining the angle between the incident and diffracted beam collimator axis constant. Bacon (Ba 55a) further shows that in the case of neutron diffraction, where the coefficient of linear absorption is small compared to that for x-ray in almost all materials, the considerably increased depth in the crystal through which diffraction occurs causes the form factor R' to become essentially independent of scattering lengths, temperature, etc., and approach a constant value of approximately three times the angular spread of the mosaics in the crystal. In current practice the dispersion of the planes of the mosaics is assumed to have a Gaussian distribution, and the spread of the mosaics is defined as the width of the Gaussian distribution at half maximum.

If the incident beam of neutrons contains white radiation, an expression for the distribution of energies in this beam is helpful. In the experiment reported here, the beam originates in the LPTR reactor core and passes through a layer of beryllium reflecting elements. In addition, the element immediately inside the beryllium reflectors on the beam axis is a regulating rod rather than a fuel element. Because of this configuration, the low energy radiation emerging in the beam is considered to approximate a Maxwellian distribution. Thus

$$I_1' = \frac{2I_1}{\lambda} \left(\frac{E}{kT}\right)^2 e^{-E/kT} , \tag{5}$$

where I_1 is the total intensity of thermalized radiation in the beam, and λ and E the wavelength and energy, respectively, of the neutrons

considered, k is Boltzmann's constant, T is the temperature corresponding to the mean transitional kinetic energy of the thermalized neutrons, and I_1' is the intensity of the neutrons of wavelength λ to $(\lambda + d\lambda)$. The intensity of the diffracted beam may therefore now be expressed as:

$$I_2' = \frac{2I_1}{\lambda}\left(\frac{E}{kT}\right)^2 e^{-E/kT} R' \, 2d \cos \theta , \qquad (6)$$

or

$$I_2' = 6I_1 \eta \left(\frac{E}{kT}\right)^2 e^{-E/kT} \cot \theta , \qquad (7)$$

where η is the mosaic spread of the crystal.

C. Construction of the Spectrometer

The spectrometer consists primarily of three sections, collimation, diffraction crystal, and spectrometer arm. Construction of the spectrometer proceeded in stages as various components were prepared. Although the spectrometer is somewhat rudimentary in design and construction, particularly in its initial forms, experimentation was carried on throughout the various construction phases. Figure 1 shows the arrangement of the principal components of the spectrometer as seen from above.

In the first stage the initial collimation was placed into position, the lead crystal mounted, and shielding placed to provide for a single angle of neutron reflection (2θ) of 36°, which corresponds to a primary neutron energy of about 0.026 electron volts. The initial collimation was placed in a 6-inch beamport facility in the shielding of the LPTR. First 6 inches of lead were placed in the port next to the core of the reactor to lower the gamma radiation level in the emerging beam. Next to the lead a circular collimator 2-3/16 in. inside diameter and 30 in. long of heavy concrete was inserted. A 21-3/8 in. gap was then left for a lead shutter provided as a part of the beam port facility. This is followed by a second collimator 1-1/2 in. square and 41 in. long of heavy concrete. Both collimators are lined on the inside with steel. This arrangement fills the beam port facility from the core to the outer face of the reactor shielding. An 8-in.-wide channel lined with 2 inches of lead was provided from the face of the reactor to the diffracting crystal. The lead crystal,

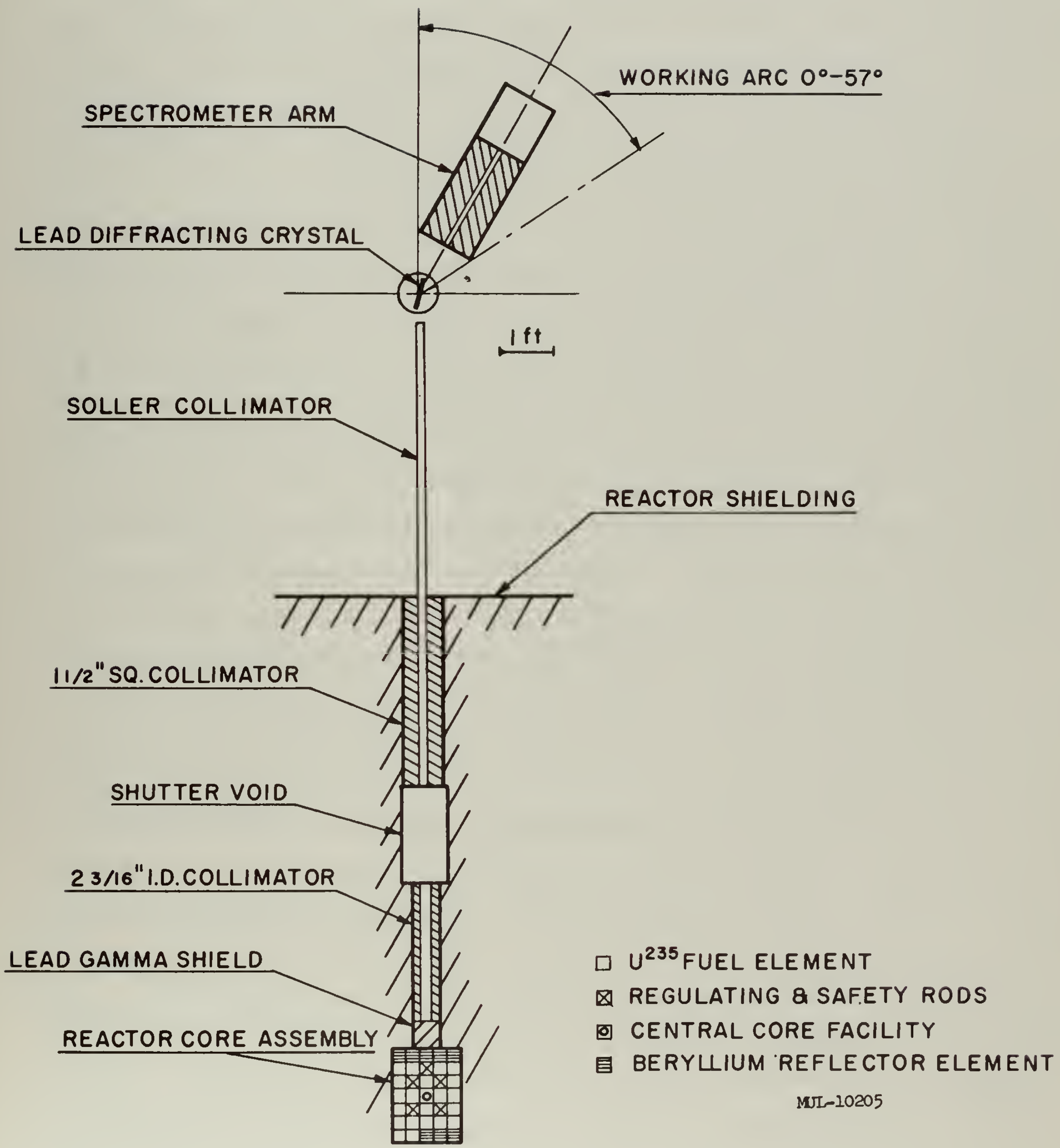

Fig. 1. Spectrometer assembly.

1/4 × 2 × 7in., mounted in an aluminum frame, was placed on a rotary table of a commercial milling machine at a position 6 feet from the outer face of the reactor shielding, so as to intercept the emerging beam. This excess distance is required to provide access to adjacent reactor facilities. The crystal was grown so that the 1, 1, 1 planes were approximately parallel to the large faces (Me 59) and obtained on loan from Dr. Warren Mead and Dr. Joseph Sparks of this laboratory. The crystal was so placed that the 1, 1, 1 planes are used for diffraction by the reflection mode. The rotary table was mounted and leveled so as to provide for positioning the vertical axis of rotation in the horizontal plane. By use of an extension control of the rotary table to the exterior of the experimental shielding, the crystal can be rotated to facilitate diffraction at any desired Bragg angle. Shimming between the crystal frame and the rotary table is required to provide for diffraction in the horizontal plane. Setting of the crystal angle is accurate to about ± 1 minute using the external control. No spectrometer arm was provided in the initial stage. The shielding was arranged to provide a channel for the diffracted beam 36° from the incident beam as noted above. While the spectrometer existed in this stage of construction a number of different detectors were tested in order to determine suitability for use in this experiment.

The second stage of construction added the spectrometer arm. The addition of the spectrometer arm provides for selection of a primary energy in the neutron beam. The spectrometer arm is supported over the crystal so that it pivots about the same axis as the axis of rotation of the rotary table. The spectrometer arm is about 4 feet long. The first 12 inches are used in a cantilever to reach the pivot support, this section riding over the crystal mounting. A 1-in.-wide, 3-in.-high, and 24-in.-long cadmium-lined collimator follows, constructed of masonite shielding material. The remaining space is available for support of the detector system. The spectrometer arm rests on an aluminum plate. The aluminum plate is scribed and aligned to within 1 minute with the incident beam from the reactor to provide indication of the angle of the spectrometer arm from the incident beam. Accuracy of placement of the spectrometer arm on the plate is ± 1 minute. With the use of a lead crystal, the

usable arc of the spectrometer (0°–57°) provides a practical primary energy range of 0.012 to 0.150 ev. The upper limit is determined by the resolution of the system, increased resolution extending the upper limit of the practical energy range as well as providing better energy definition throughout the range.

The third stage of construction consisted of the addition of collimating septa to provide finer collimation of the incident neutron beam in an arrangement similar to the Soller collimator first used in x-ray studies. The new collimator contains eleven channels 0.125 in. wide, 1 in. high, and 77 in. long, separated by 0.012-in. aluminum separators. It was originally intended that this collimator would be inserted into the 1-1/2 in. square collimator to the shutter space, and extend outward to within a few inches of the diffracting crystal. During the initial attempt at installation it was found that the internal dimensions of the 1-1/2 in. square collimator had decreased by about 0.020 in. since preparation and the collimator insert would not fit properly. Modifications to the collimator insert were made; this collimator, as now installed, extends 17 in. into the 1-1/2 in. square collimator and outward to about 6 in. from the crystal center.

In the first two stages of construction, the dispersion of the incident neutron beam was sufficient to bathe the lead crystal completely at all angles of diffraction available. Thus the collimation of the incident beam is dependent on the crystal angle. The effective full-width dispersion of the incident beam amounts to:

$$D = 2 \arcsin\left(\frac{1.094 + 3.50 \sin \theta}{164.375}\right). \qquad (8)$$

In the practical range of the spectrometer, this full-width dispersion of the incident beam varies between 1° 6' at the high energy end and 1° 52' at the low energy end. The addition of the 77-inch collimator insert provides for a constant collimation of the incident beam. The full-width dispersion of the incident beam is now 11' 00''.

When the width of the incident beam at the lead crystal position is wider than the apparent width of the crystal presented to the beam, the intensity of the diffracted beam will be proportional to the width of the crystal presented to the incident beam (ignoring beam distribution):

$$I_2' \propto I_1' \sin\theta \, . \tag{9}$$

Combining this with Eq. (7), the intensity of the diffracted beam may be re-expressed as:

$$I_2' \propto 6I_1\eta\left(\frac{E}{kT}\right)^2 e^{-E/kT}\cos\theta \, . \tag{10}$$

With the addition of the new collimator, this will be true only when the apparent width of the crystal to the incident beam is less than the width of the collimator. Thus after this additional collimation is added, Eq. (7) for the intensity of the diffracted beam will be valid for crystal (Bragg) angles greater than 12° 22′ and Eq. (10) will be valid for crystal angles less than 12° 22′ as:

$$I_2' = \frac{6I_1\eta}{\sin 12° \, 22'}\left(\frac{E}{kT}\right)^2 e^{-E/kT}\cos\theta \, .$$

D. Resolution

In order to make a rough determination of the spectrometer resolution and second-order contamination of the diffracted beam, a number of rocking curves were prepared at points throughout the spectrometer range after the spectrometer arm had been added. The rocking curve is prepared by positioning the spectrometer arm at a particular angle and measuring the intensity of radiation reflected down the arm as the diffracting crystal is rotated through the Bragg angle for the spectrometer arm setting. The curve resulting from the plotting of intensity vs crystal angle is a function of the angular distribution of the incident radiation (usually a triangular function) and the angular distribution of the crystal mosaics (commonly assumed to be Gaussian). As a first approximation, the energy width at half maximum of this curve divided by the energy of the peak may be equated to the resolution of the spectrometer ($\Delta E/E$). The width at half maximum of the resolution function (ΔE) is a function of the energy, being expressed approximately by $\Delta E = kE^{3/2}$, where k is a constant of the spectrometer. Complications entering at low energy cause a departure from this approximate rule (Sa 56). This spectrometer constant may be expressed in terms of the uncertainty in time of flight

divided by the length of the flight path. For a figure of merit K in units of microseconds per meter, $K = 36.15\ \Delta E/E^{3/2}$, where $\Delta E/E^{3/2}$ is in units of $(ev)^{-1/2}$.

To obtain data for the rocking curves a 1 in. diam BF_3 counter was placed on the spectrometer arm at the end of the 1 - × 3 in. channel in an end window configuration. A cadmium shutter with a 3/16 in. vertical slot was placed in front of the BF_3 counter to restrict the sample area and more closely define the spectrometer arm setting. Data for rocking curves was taken at several spectrometer arm settings throughout the range of the spectrometer. One-minute runs were made at each crystal setting. The crystal setting was varied in 15' steps through the region of the Bragg diffraction peak. From this data rocking curves were constructed for each spectrometer arm setting.

The rocking curves constructed in this attempt at determining the resolution of the spectrometer show an anomaly which is not yet fully explained. The rocking curves described above can be expected to show approximately a Gaussian form. The angular setting of the crystal at the peak of a rocking curve can be expected to vary quite accurately at exactly half the rate at which the angular setting of the spectrometer arm varies. The rocking curves at the high and low energy end of the spectrometer range appeared satisfactory in form, however those in the center of the spectrometer range exhibited double peaks. The position of the crystal at the main peak varied from that expected at many of the points observed. As the energy of the spectrometer arm setting increases, the secondary peak first appears on the low energy side of the rocking curve, rises in amplitude to that of the main peak, and then decreases in amplitude, lowering on the high energy side of the rocking curve. The distance between the two peaks corresponds to a change in the crystal setting of about 30'. For further study the slotted cadmium shutter was replaced by one containing a circular aperture 0.1 cm^2 in area. The characteristic of a rocking curve taken with this shutter at a primary diffraction energy of 0.03 ev can be seen in Fig. 2. The difference between the crystal settings at the peaks of the rocking curves taken at the

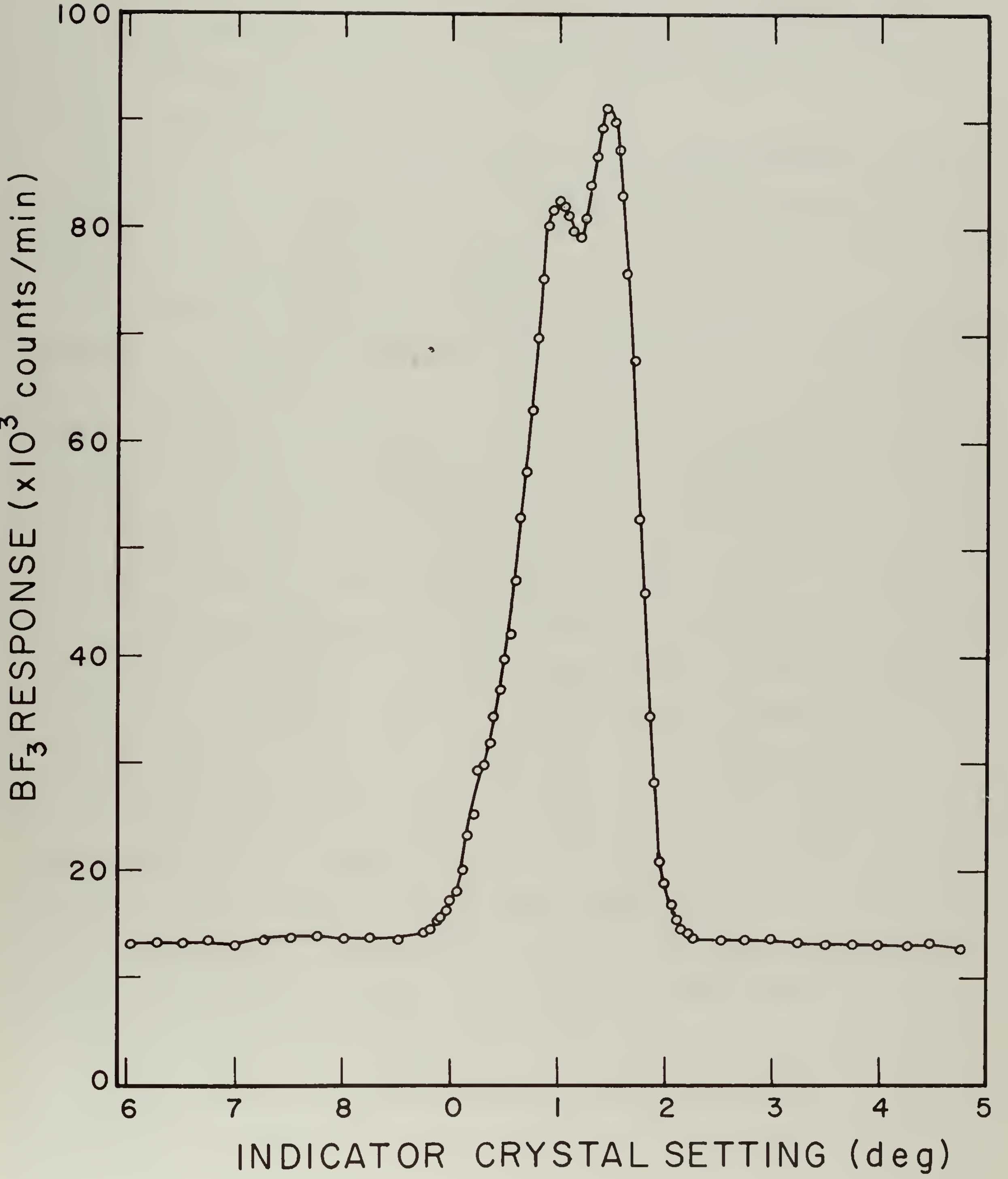

MUL-10206

Fig. 2. Rocking curve at 0.03 ev.

four highest energy points is exactly half the difference between the spectrometer arm settings at those points, as should be expected. These four points were used as a basis for establishing the zero angle position of the crystal planes used for diffraction with the incident beam on the crystal adjustment scale.

Some other characteristics of these curves, and resolution figures for the spectrometer at the several energy points, are shown in Table I. Note that the anomaly of the second peak is reflected in the values of resolution obtained from these rocking curves.

Three possible explanations suggest themselves for this double peak phenomenon. The first is that the diffracting crystal is not a single crystal of mosaics, but broken into two such crystals with a linear displacement of about 30'. The second is that the beam emerging from the 1-1/2 inch square collimator contains two more finely collimated and intense sections, the axes of which are displaced horizontally by about 30'. The third is that 30' reflections are occurring on the wall of the collimator. The second and third explanations seem doubtful at first consideration, but a comparison of the predicted and observed crystal angles of the peaks fails to show a 30' shift in the peak. If the crystal did exhibit lineage structure, it might more likely be expected that one lineage would predominate initally. Then as the spectrometer arm setting was changed to correspond to differing energies, changes in the Bragg angle required of the crystal would bring the second lineage into predominance. In this case, there would be a definite shift of 30' in the position of the observed peak from that predicted (based on initial positions of the first few peaks) when the second peak became more dominant. This shift is not apparent in the data tabulated. For this reason, the first investigations of this anomaly were centered on the incident beam.

A new rocking curve was taken at a spectrometer setting for 0.030 ev, a point at which the anomaly had been observed previously. The crystal setting was changed in 3' steps. A 1/10 cm^2 aperture was placed before the BF_3 in counter place of the slotted shutter to reduce a high count rate previously observed. This resulted in the more detailed curve

Table I. Spectrometer Resolution Data

Primary neutron energy (ev)	Predicted crystal angle at peak	Observed crystal angle at peak	Resolution	
			ΔE/E	K (μsec/m)
0.0125	26° 36'	26° 45'	0.0640	20.68
0.015	24° 07'	24° 11'	0.0734	21.63
0.020	20° 43'	20° 53'	0.1050	26.83
0.025	18° 27'	18° 38'	0.1360	31.09
0.030	16° 48'	16° 57'	0.1400	29.22
0.035	15° 31'	15° 38'	0.1400	27.06
0.040	14° 29'	14° 29'	0.1500	27.11
0.050	12° 56'	12° 41'	0.1480	23.93
0.060	11° 47'	11° 37'	0.1616	23.86
0.070	10° 54'	10° 45'	0.1515	20.68
0.080	10° 11'	10° 08'	0.1363	17.41
0.090	9° 36'	9° 32'	0.1345	16.21
0.100	9° 06'	9° 03'	0.1280	14.63
0.110	8° 41'	8° 40'	0.1364	14.86
0.120*	8° 18'	8° 18'	0.1133	11.82
0.130*	7° 59'	7° 59'	0.1123	11.26
0.140*	7° 41'	7° 41'	0.1214	11.73
0.150*	7° 25'	7° 25'	0.1400	13.07

*The consistency of the angular position of the diffracting crystal at the peak reflection with the spectrometer arm position at these four points was used to establish the position of zero cyrstal angle for the observed crystal position data.

reproduced in Fig. 2, showing a well-defined double peak. Then a 1/16 in. thick cadmium plate with a 1 in. diam circular aperture was placed over the outside end of the 1-1/2 in. collimator so that the circular aperture was centered about the axis of the collimator. With this plate in place to reduce collimator wall effects, the rocking curve was repeated. The secondary peak again was readily apparent and well defined, but slightly reduced in relative amplitude. The 1 in. aperture was then replaced with a 3/8 in. diam circular aperture. Similar runs were then repeated with this aperture at the center of the collimator exit, near the left side of the collimator exit, and near the right side of the collimator exit. With the aperture in the center and left side of the collimator exit, the anomaly was no longer observed. However, when the aperture was moved to the right side the anomaly returned very strongly, with the amplitude of the secondary peak rising to twice the amplitude of the former primary peak. Since, with this aperture at the collimator exit, the beam had sufficient room to spread out to cover the entire crystal, it is felt that the double peak anomaly is probably due to the second explanation: that the incident beam from the reactor contains two major axes of emanating radiation. Should this be true, further substantiation would be provided upon insertion of the Soller collimator, which more closely defines the beam emanating from the reactor incident upon the crystal. With this definition of the beam and explanation of the anomaly, the secondary peak should disappear entirely.

The recent addition of the Soller collimator to the spectrometer has caused the second peak to disappear. After installation, the series of rocking curves was repeated, using the 0.1-cm^2-aperture shutter shielding the BF_3 counter. Additional points up to 0.19 ev were added and no evidence of the secondary peak effect was observed. Resolution of the new system is shown by the data in Table II and in Fig. 3. The total error accumulated in counting, and in the plotting and reading of graphs used in the determination of these resolution values, is estimated to be about 10% of the final value obtained.

From Fig. 3 an average value for the resolution figure of merit (K) of 13 μsec/meter is obtained for the instrument in its present form.

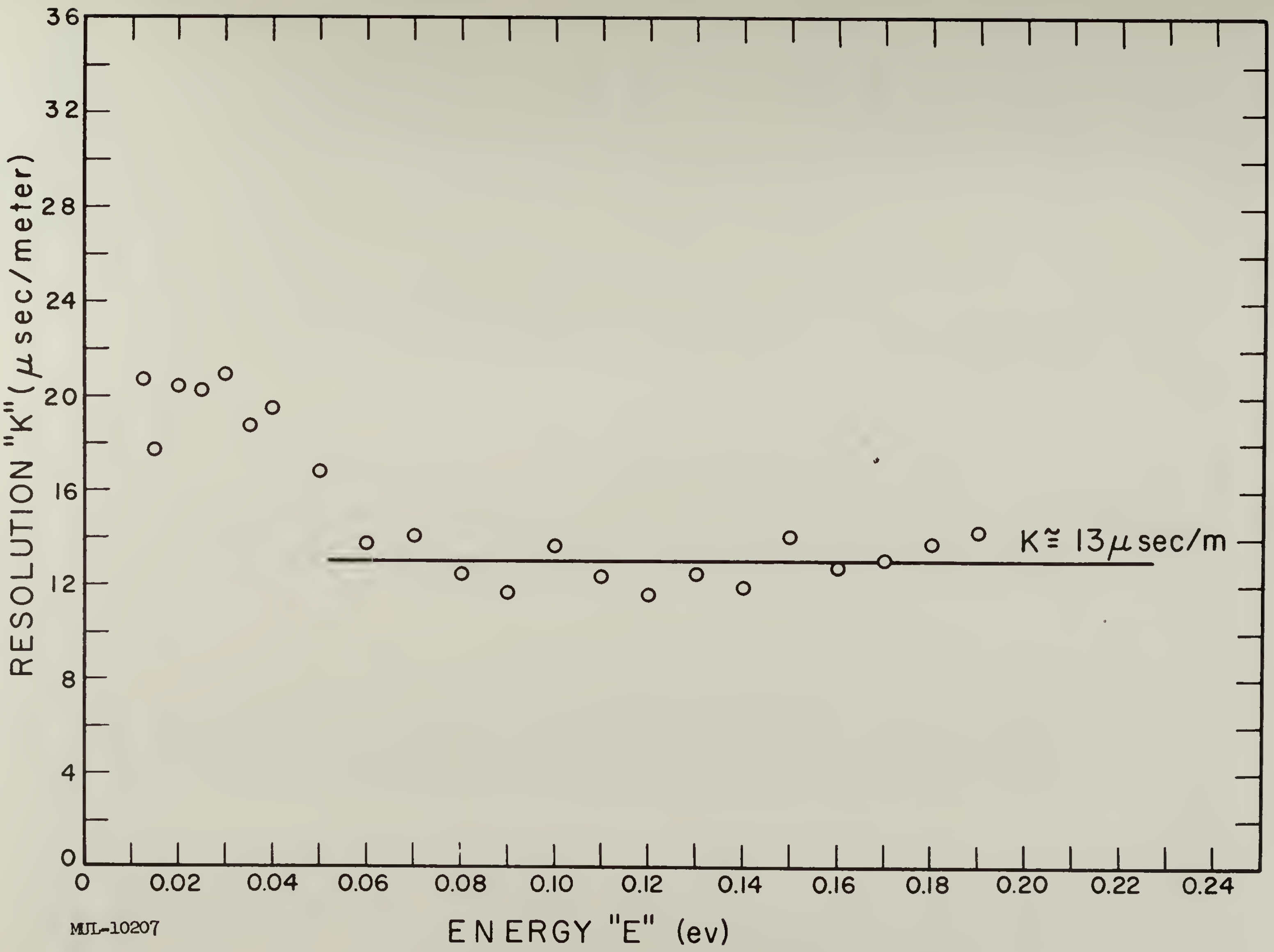

Fig. 3. Resolution figure of merit "K".

Table II. Spectrometer Resolution Data

Primary neutron energy (ev)	Predicted crystal angle at peak	Observed crystal angle at peak	Resolution	
			ΔE/E	K (μsec/m)
0.0125	26° 36'	26° 41'	0.0640	20.68
0.015	24° 07'	24° 14'	0.0600	17.70
0.020	20° 43'	20° 52'	0.0800	20.43
0.025	18° 27'	18° 37'	0.0880	20.11
0.030	16° 48'	17° 01'	0.1000	20.87
0.035	15° 31'	15° 45'	0.0972	18.77
0.040	14° 29'	14° 40'	0.1075	19.42
0.050	12° 56'	13° 07'	0.1040	16.81
0.060	11° 47'	11° 55'	0.0934	13.77
0.070	10° 54'	10° 59'	0.1029	14.05
0.080	10° 11'	10° 16'	0.0975	12.45
0.090	9° 36'	9° 41'	0.0967	11.65
0.100	9° 06'	9° 10'	0.1200	13.71
0.110*	8° 41'	8° 41'	0.1136	12.39
0.120*	8° 18'	8° 19'	0.1125	11.74
0.130*	7° 59'	7° 59'	0.1246	12.49
0.140*	7° 41'	7° 41'	0.1235	11.94
0.150*	7° 25'	7° 24'	0.1507	14.06
0.160*	7° 11'	7° 11'	0.1413	12.76
0.170*	6° 58'	6° 57'	0.1495	13.10
0.180*	6° 46'	6° 47'	0.1611	13.73
0.190*	6° 36'	6° 36'	0.1721	14.27

*The consistency of the angular position of the diffracting crystal at the peak reflection with the spectrometer arm position at these nine points was used to extablish the position of zero crystal angle for the observed crystal position data.

Sailor et al. (Sa 56) have established a criterion for estimating the ability of a spectrometer to resolve and analyze resonances, based on an average heavy isotope. Resolution is obtained if the spectrometer resolution function (ΔE) is less than 3 ev, and analysis may be adequately performed when the function is less than 0.1 ev. Using this criterion, the figure of merit of 13 μsec/m provides for the resolution of resonances occurring below 4-ev neutron energy and for the analysis of resonances below 0.4-ev neutron energy.

Calculations of the relative intensity of the neutron beam incident on the diffracting crystal by the method of Szabo (Sz 59) show that the intensity of this beam upon installation of the Soller collimator should be reduced to 10.5% of its intensity before installation. This is borne out by a comparison of the incoherent scattered background before installation (135,000 c/cm^2 min) and after installation (16,000 c/cm^2 min). However the reduction in the intensity of the coherently scattered neutrons of the Bragg diffraction peak is considerably less, dropping from a relative value of 915,000 c/cm^2 min to 260,000 c/cm^2 min at the 0.030-ev spectrometer setting. Thus the addition of the Soller collimator has appreciably improved the signal-to-noise ratio.

One further discrepancy is apparent from Table II, namely, a deviation of the position of the observed peak from that predicted. Again the observed crystal positioning scale readings were converted to the position of the crystal planes with respect to the incident beam by the consistency in the angular difference between energy peaks with the change in the spectrometer arm setting. Very close consistency was observed at the nine highest energy positions observed. However, as the spectrometer arm angle is increased a discrepancy occurs in the observed peak position from that predicted, the difference between the two increasing to 14' at 0.035 ev and then decreasing again. A great amount of care was taken in the alignment of this apparatus and this discrepancy is well outside the expected limits of error from alignment inaccuracies. Nonetheless, alignment is the first consideration as the probable cause of a discrepancy of this type. Further investigation of this problem will be made.

E. Harmonic Contamination

One of the complications which accompany diffraction spectrometers of this type is the harmonic contamination of the reflected beam by diffractions of higher order. The wavelengths of these harmonic neutrons are defined in the Bragg equation for values of n greater than 1. This harmonic contamination is of appreciable amplitude in the thermal region, and in order to compensate for it in making measurements with the spectrometer, the harmonic contamination must be determined. A method for the determination of second-order contamination is described by Haas and Shore (Ha 59). Because of the sharp decline in intensity of the harmonic contaminations with increasing order, correction for higher orders is not considered necessary at present.

Calculation of the second-order effect from the data obtained prior to insertion of the Soller collimator was not attempted nor felt warranted due to the unexplained double-peak anomaly. A continuation of the rocking curve data obtained to higher energies after insertion of the Soller collimator will provide an estimate of the second-order effect by the method of Haas and Shore. Two parameters of this determination which are not yet known accurately are the mosaic spread of the lead diffracting crystal and the temperature that corresponds to the mean transitional kinetic energy of the thermalized neutrons. It is felt that an iterative process of curve matching, using second-order calculations as above and the primary estimate based on Maxwellian neutron distrubution [Eq. (10)], may be able to resolve these parameters.

As a graphic illustration of the second-order contamination, the BF_3 counter response at the peaks of the rocking curves at the several energies measured is shown plotted against energy in Fig. 4. Although the BF_3 counter efficiency is not yet accurately known, it is felt to be flat with respect to the energy. Two primary reflection approximations using Eq. (10) and normalized to 95% of the response to the peak at 0.18 ev are also shown. The full line shows tht predicted primary radiation level corresponding to a neutron temperature of 305°K, the exit temperature

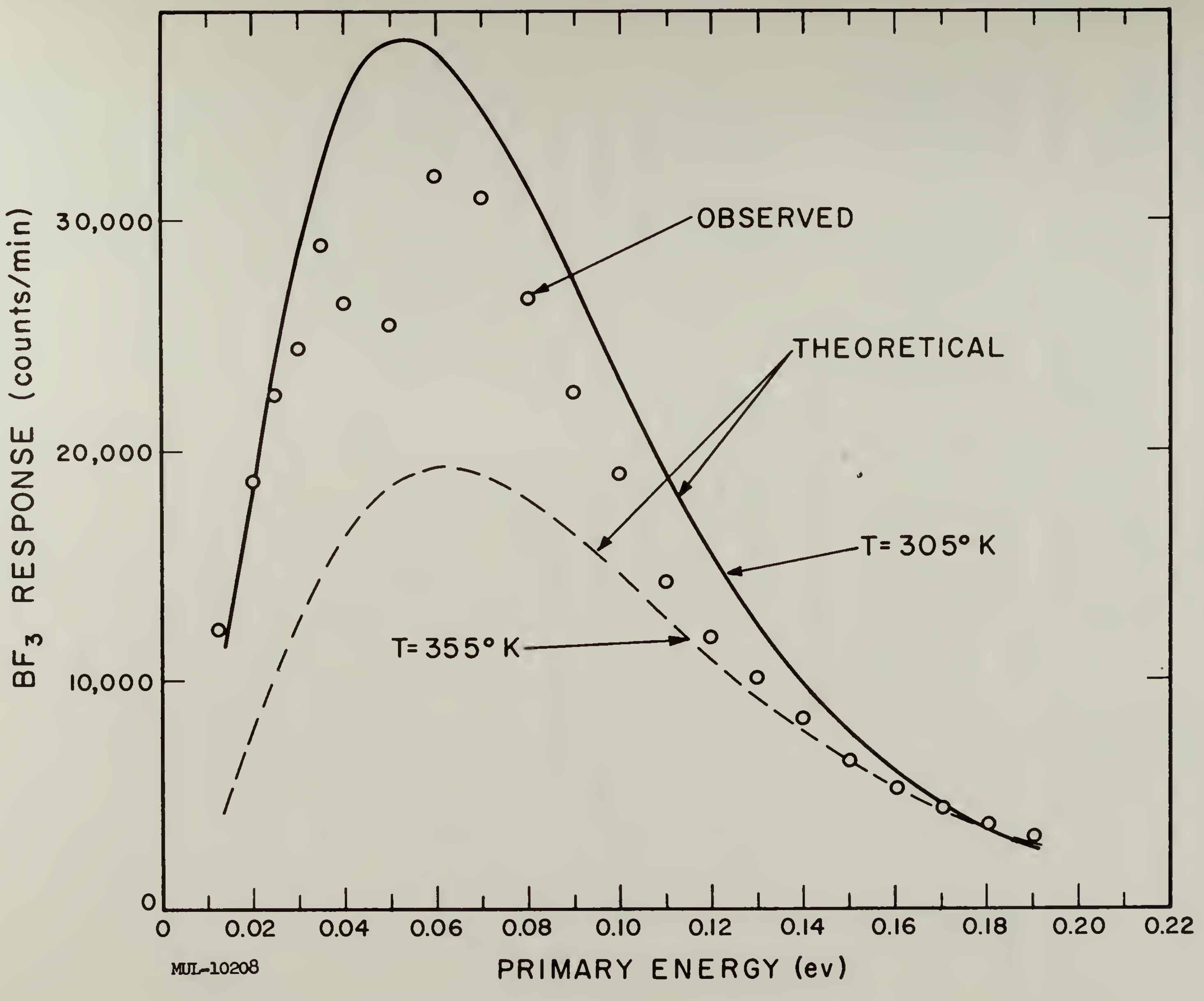

Fig. 4. Diffracted neutron intensity (with first-order approximations).

of the reactor cooling water. The dashed line shows the predicted primary intensity corresponding to 355°K, 50°C higher than the exiting water temperature. Bacon (Ba 55a) uses an even higher temperature estimate (375°K) in discussions concerning pile neutrons.

The sharp discontinuity in observed peak intensity at 0.04 and 0.05 ev shown in Fig. 4 corresponds to the position where the ends of the lead crystal are being exposed to the incident beam. A similar discontinuity was observed prior to the insertion of the Soller collimator and was thought then to accompany the double-peak anomaly. This discontinuity will have to be the subject of further investigation.

III. BERYLLIUM-7 HANDLING

The beryllium-7 isotope is produced in a cyclotron by the $Li^7(p, n)Be^7$ reaction. It is obtained from commercial sources in the form of the chloride dissolved in a 1<u>N</u> solution of hydrochloric acid. In this form it could not readily be incorporated with a number of the scintillation detecting mediums thus far used. Also, in the very small amounts to be used (of the order of 10^{-9} gram) transfer losses were feared. A substitute form, suggested by Dr. G. M. Iddings of this laboratory, has been utilized in the experiment up to this time. In this form the Be^7 is bound in an organic chelating agent, thenoyl-trifuoro-acetone, $C_4H_3SCOCH{:}C(OH)CF_3$. The Be^{7++} radical substitutes for the OH^- radical, joining two of the organic molecules in a covalent bonding. In this form the beryllium is chemically very stable and easily transferred from one medium to another with small losses (Id 59). Another advantage lies in the fact that the additional chelating material, not joined with the beryllium, can be easily separated out chemically. The transfer of the beryllium into the chelate form for this experiment has been performed by Dr. Iddings with each lot received.

The beryllium chelate has one disadvantage in that it exhibits a strong orange coloring. Even in the very small amounts utilized, it has tended to discolor the detecting medium. Apparent reductions in counter efficiency have been observed in some instances. Counters in which other forms of the beryllium will be more appropriate are being constructed.

Identification of the Be^7 and determination of the amount present in the several samples used, were made from observations of the characteristic 478-kev gamma ray. Radioactive contaminants in the Be^7 were not observed. Data for these determinations were taken with a 3- × 3-inch NaI(Tl) crystal detector system assembled by Dr. Walter John and Cdr. Morris Prosser, USN. The estimated error in the determination of the amounts of Be^7 present by this method is ±15%, the major factor of which is the 10% uncertainty in the branching ratio of Be^7 decay. Observations of the 53.4-day half-life for identification were not made in the initial stages of the experiment due to transfers of Be^7 from one detector to another with resultant losses. Assuming some losses in transfer, the 53.4-day half-life is commensurate with the decay observed in the samples.

IV. DETECTORS

A number of types of detectors have been and are under consideration to detect the $Be^7(n,p)Li^7$ reaction. Most have proven unsatisfactory; with only one has the reaction been observed. In all types thus far used the attempt has been to detect and identify the recoil proton.

A. Nuclear Emulsions

The first detecting medium tried was the nuclear emulsion. Ilford C-2 plates of 50-micron emulsion thickness were used for their property of relative gamma insensitivity. The plates were cut to 1- × 1-inch size. Ten plates were brushed with a very weak solution of H_3BO_3, the amount chosen to approximate the event rate expected from the Be^7 concentrations which were to be available. The plates were humidified for five hours in a moist atmosphere to enhance diffusion of the H_3BO_3 throughout the emulsion, then dried and wrapped. Runs were made in the Livermore Water Boiler Reactor and in the LPTR at several points calculated to produce one to ten events per field of view of the scanning microscope. In all cases, the time for exposure was so long that darkening of the plates due to gamma radiation was excessive and accurate reading of the plates

impossible. This method was finally abandoned, as it was felt that the Be^7 in the emulsions would enhance the darkening effect. The films would be exposed to the Be^7 a number of additional hours during preparation and processing as well as during the reactor exposure time. It appeared doubtful that proper conditions of high neutron flux and low gamma-ray intensity could be achieved.

B. Plastic Scintillators

Attempts were made to develop a 4π scintillation crystal by depositing a thin layer of the target material in a sandwich between two scintillating crystals and dissolving the interior surface. Again, initially, boric acid was used as the target material. The ultimate size of the finished crystal was to be 1 in. in diameter and 0.020 in. thick. It was hoped that the gamma-ray sensitivity of such a thin crystal would be low enough so that the desired recoil prontons could be observed. The material chosen was a commercial polystyrene plastic scintillation material. Samples were obtained in 0.030, 0.020, and 0.010 in. thickness.

Satisfactory joining of the crystals was not obtained. A number of solvents were tried, and styrene monomer as well. Combinations of solvents and heat, and heat alone, were attempted. Almost all crystals turned out cloudy or became cloudy within a few hours after binding. The primary cause of cloudiness appeared to be stress relief in the plastic, as many times it appeared to be formed by many minute cracks in the material. Some cloudiness was not attributable to these cracks and could only be assumed as due to a chemical change or incomplete binding.

Four of the more promising crystals were exposed to a diffracted neutron beam. Three contained H_3BO_3 in differing amounts, while the fourth was used as a control. Pulse-height analysis of the crystal response was made with a 256-channel analyzer. Results indicated no difference not attributable to efficiency reduction by clouding. The gamma background amounted to about 25,000 counts per second. An estimated boron event rate of 16,000 events per second was not observable, indicating very poor efficiency for detecting this reaction.

A small sample of Be^7 was also placed on a 0.010-in. plastic scintillating arrangement and irradiated for a period sufficient to produce an estimated 3000 $Be^7(n,p)Li^7$ events. No concrete evidence of these events could be observed in the gamma background. The experiment was repeated using a thin CsI(Tl) crystal, with identical result.

C. Liquid Scintillators

In order to reduce the background count, an anticoincidence system was devised using a liquid scintillator. The scintillator material used was a mixture of 1000 grams of phenylcyclohexane, 4 grams of P-terphenyl, and 38 milligrams of diphenylhexatriene. The detector consisted of two liquid scintillator chambers 1/16 in. thick by 3/4 in. diameter separated by a 0.002 in. aluminum foil. One chamber was loaded with the liquid scintillator to which a small amount of Be^7 chelate had been added. The other chamber was loaded with the plain liquid scintillator. The plain scintillator was observed directly by a 6199 photomultiplier tube, the Be^7-loaded scintillator being observed through a lucite prism, as is shown in Fig. 5.

The preamplifier circuitry was designed to take two signals from the photomultiplier tube, that is, a "fast" signal from the final stage dynode and a "slow" signal from the dynode four stages previous to this. The tube was operated under such conditions that the slow signal, originating at an earlier dynode, was approximately linear with the magnitude of the light pulse, while the fast signal, originating at the final dynode was overdriven to a great extent. The fast signals resulting were of uniform height and shape regardless of the magnitude of the original light pulse and were used to establish coincidence between the two sides of the crystal. This coincidence signal was then used as an anticoincidence base on the linear slow signals emanating from the Be^7 side of the crystal. The final anticoincidence signal was then used to gate a scaler and 256-channel analyzer.

Considerable alignment of the electronic system was required. After several attempts the maximum fast-signal coincidence counting rate

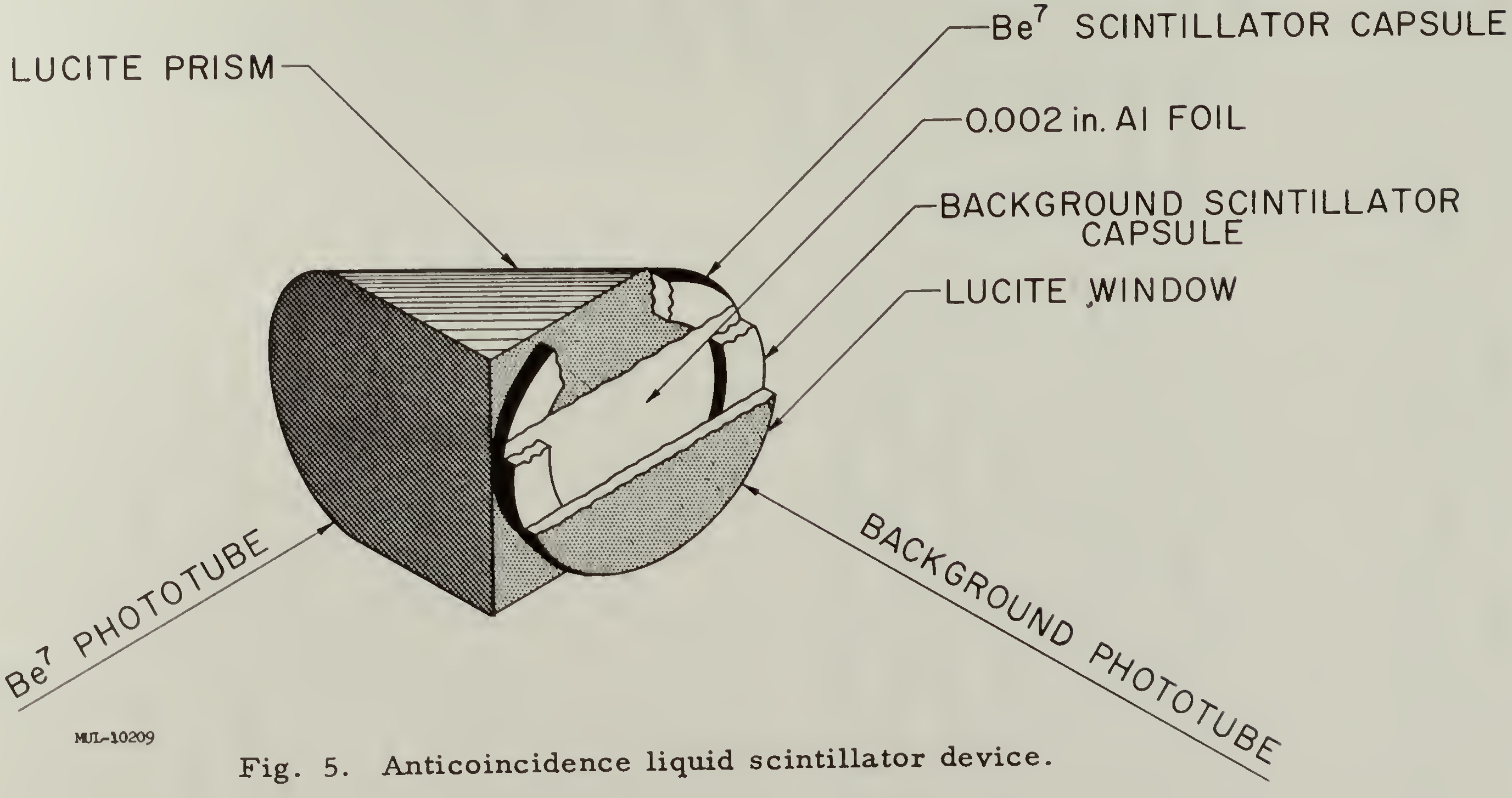

Fig. 5. Anticoincidence liquid scintillator device.

accounted for less than 20% of the total counting rate from one photomultiplier system. This was not sufficient to lower the background to a satisfactory level. ZnS(Ag) crystals had begun to show some promise at this time and study of the liquid scintillator system was temporarily discontinued.

D. Zinc Sulfide

Silver-activated zinc sulfide has the particular properties of being sensitive to protons and heavier charged particles, while relatively insensitive to gamma and beta radiations. Unfortunately, in the microcrystalline form, it also has rather poor resolution due to diffuse light scattering, energy losses in air between crystals, and a high opacity to its own radiation (ZnS(Ag) is essentially opaque at 80 mg/cm^2 to its own radiation) (Ke 54). In addition, ZnS(Ag) is neutron sensitive to both thermal and fast neutrons by a number of reactions, the most important of which occur with sulfur:

$S^{32}(n, p)P^{32}$ $\quad Q = -0.93$ Mev $\quad \sigma_f = 3$ barns

$S^{32}(n, \alpha)Si^{29}$ $\quad Q = 1.521$ Mev $\quad \sigma_{th} = 1.8 \pm 1.0$ mb

$S^{33}(n, p)P^{33}$ $\quad Q = 0.533$ Mev $\quad \sigma_{th} = 125 \pm 100$ mb

$S^{33}(n, \alpha)Si^{30}$ $\quad Q = 3.494$ Mev $\quad \sigma_{th} = 8$ mb .

The cross sections for these reactions are sufficiently high and the amount of Be^7 available so minute that the event rates are of equivalent or greater magnitude in the thermal region. Nonetheless, preliminary results indicate that the Be^7(n, p)Li^7 reaction can be observed in ZnS(Ag).

Thin aluminum cups 0.005 to 0.015 in. deep were prepared to hold the ZnS(Ag) powder. In order to reduce spillage and assist the ZnS(Ag) in holding its shape in the cup, the ZnS(Ag) was placed in the cup, smoothed to a uniform layer and then moistened with methyl alcohol. After the alcohol had evaporated, it was found that the ZnS(Ag) tended to hold its shape moderately well and remain in the cup if not roughly handled.

These cups were placed on the face of a 6810A photomultiplier tube

and exposed to the diffracted neutron beam. Response of the crystal was observed on a 256-channel analyzer. The single spectrometer angle of 36° (2θ) only was available for these runs.

With thicknesses of about 40 mg/cm^2 of ZnS(Ag), two very broad peaks could be observed separated from the low pulse-height response by a saddle. One such crystal was loaded with 0.100 ml of a saturated solution of NH_4NO_3 in methyl alcohol in an attempt to see $N^{14}(n, p)C^{14}$ events (E_p = 0.586 Mev). The response of this crystal identified the first ZnS(Ag) peak as probably due to the $S^{33}(n, p)P^{33}$ reaction. The second peak rose on the tail of the first peak. This peak was assumed to result from $S^{32}(n, \alpha)Si^{29}$ and other events.

A ZnS(Ag) crystal of 40.2 mg/cm^2 thickness was then prepared and a small amount of Be^7 added. Experimentation with this crystal failed to produce a separate pulse height response peak attributable to the Be^7 reaction. On the assumption that Be^7 response might be observable in the second ZnS(Ag) response peak (1.338 Mev α), a set of comparison runs were made. The Be^7-loaded crystal was exposed to the diffracted beam for 847 minutes and the response observed on a pulse-height analyzer. 1.08×10^{-10} gram of Be^7 remained in the crystal at the time of this run. The response was plotted on semilog paper and the tail of the first peak extended under the second peak. The difference between the total counts in each channel in the region of the second peak and the counts in the same channel attributable to the first peak by this extension were tabulated. This analysis resulted in a response of 19.6 counts per minute in the second peak. A plain ZnS(Ag) crystal of 36.0 mg/cm^2 thickness was then prepared, exposed for 530 minutes and the response of this crystal subjected to the same analysis. The response of the second peak was found to be 12.7 counts per minute in this case. Correction for the difference in crystal size allows a maximum count rate of 14.2 counts per minute for a plain crystal of equal size as the Be^7 prepared crystal. This type of analysis is not necessarilly empirically satisfying; however, the change in count rate of 5.4 counts per minute compares favorably with an expected 5.5 counts per minute based on the

reported thermal cross section and does seem to be a large difference factor even for this poor an analysis.

After installation of the spectrometer arm, two 6810A photomultiplier tubes were obtained and a scintillation crystal of ZnS(Ag) 1 in. diameter and 70.6 mg/cm^2 thick prepared on the face of each phototube. A circle of adhesive cement was placed on the phototube surfaces about a 1 in. diam form to make the sustaining wall for the ZnS(Ag) crystal. One of these crystals was loaded with approximately 1 mC (2.9×10^{-9} gram) of Be^7 in the chelate form, the other was left unaltered. These crystals were prepared in an attempt to see a definite reponse to thermal neutrons by the Be^7 at several specific energies. The crystals were exposed to the diffracted neutron beam at angles corresponding to primary energies of 0.0125, 0.026, 0.050, and 0.100 ev. Runs of 250-minute duration in both the direct diffracted beam and with 0.032 in. cadmium shielding of the beam were made for both crystals at each angle. A definite response believed due to the Be^7 contamination in one crystal was observed and is discussed in Section V, "Results."

E. Additional Detectors

Two additional detectors are presently under construction. Beryllium acetylacetonate, $Be(C_5H_7O_2)_2$, is a stable form, crystalline at normal room temperature, melting at 108°C, and vaporizing at 270°C. Moljk, Drever, and Curran of Glasgow University have experimented with the use of glass proportional counters at elevated temperatures (Mo 55). An end window glass proportional counter is under construction using principles developed at Glasgow in which it is intended to vaporize beryllium-7 acetylacetonate in an argon and carbon-dioxide atmosphere by heating to 300°C or more, for exposure to the diffracted neutron beam. Problems are expected. Some similar attempts by other British investigators have been unsuccessful. (Do 59).

Experimentation is being carried out by some electronics manufacturers and in the Livermore laboratory with the use of photomultiplier tube configurations as electron multipliers (Al 47) (Ma 60). In another

detector under construction for Be^7 study, the Be^7 will be deposited on a very thin tape of Mylar, essentially transparent to protons and suspended in a vacuum chamber. An electron multiplier will be placed above the Be^7 sample to detect the recoiling Li^7 atoms. Below the sample a ZnS(Ag) crystal will be placed to observe protons through the Mylar tape. Coincidence pulses between the two detectors when the Be^7 is exposed to a thermal beam will identify the $Be^7(n, p)Li^7$ reaction.

V. RESULTS

During the testing of ZnS(Ag) as a detecting medium prior to the installation of the Soller collimator, two crystals were prepared of 70.6 mg/cm^2 thickness, one loaded with an amount of Be^7 chelate and exposed to the diffracted neutron beam at four spectrometer settings, 0.0125, 0.026, 0.050, and 0.100 ev. Four 250-minute runs were made at each setting, one for each of the two crystals exposed to the diffracted beam, and one for each of the two crystals shielded from the beam with 0.032 in. of cadmium. Pulse-height response was recorded with a 256-channel analyzer. The thermal neutron response of the crystals (that is, open beam response with cadmium shielded response for the same crystal subtracted) is plotted by channels for the Be^7-loaded crystal and the unloaded crystal at each of the energy points observed in Figs. 6 through 9. Because of the double-peak anomaly present in the beam at this time, a detailed analysis of the results was not attempted; however, certain aspects of the recorded data are significant and bear mention.

In general, the low-level response of the Be^7-loaded crystal is less than the response of the unloaded crystal, reflecting the previously observed decrease in efficiency observed on the adding of the Be^7 chelate. The amount of this loss of efficiency will depend on the amount of contaminant applied and was not determined in this instance. An increase in the pulse-height response in the Be^7-loaded crystal at the 28-30 volt level over that of the unloaded crystal is noted at all four energies. This increase is particularly marked at the 0.026-and 0.050-ev energy settings. It is considered that the area between the responses in this region is a

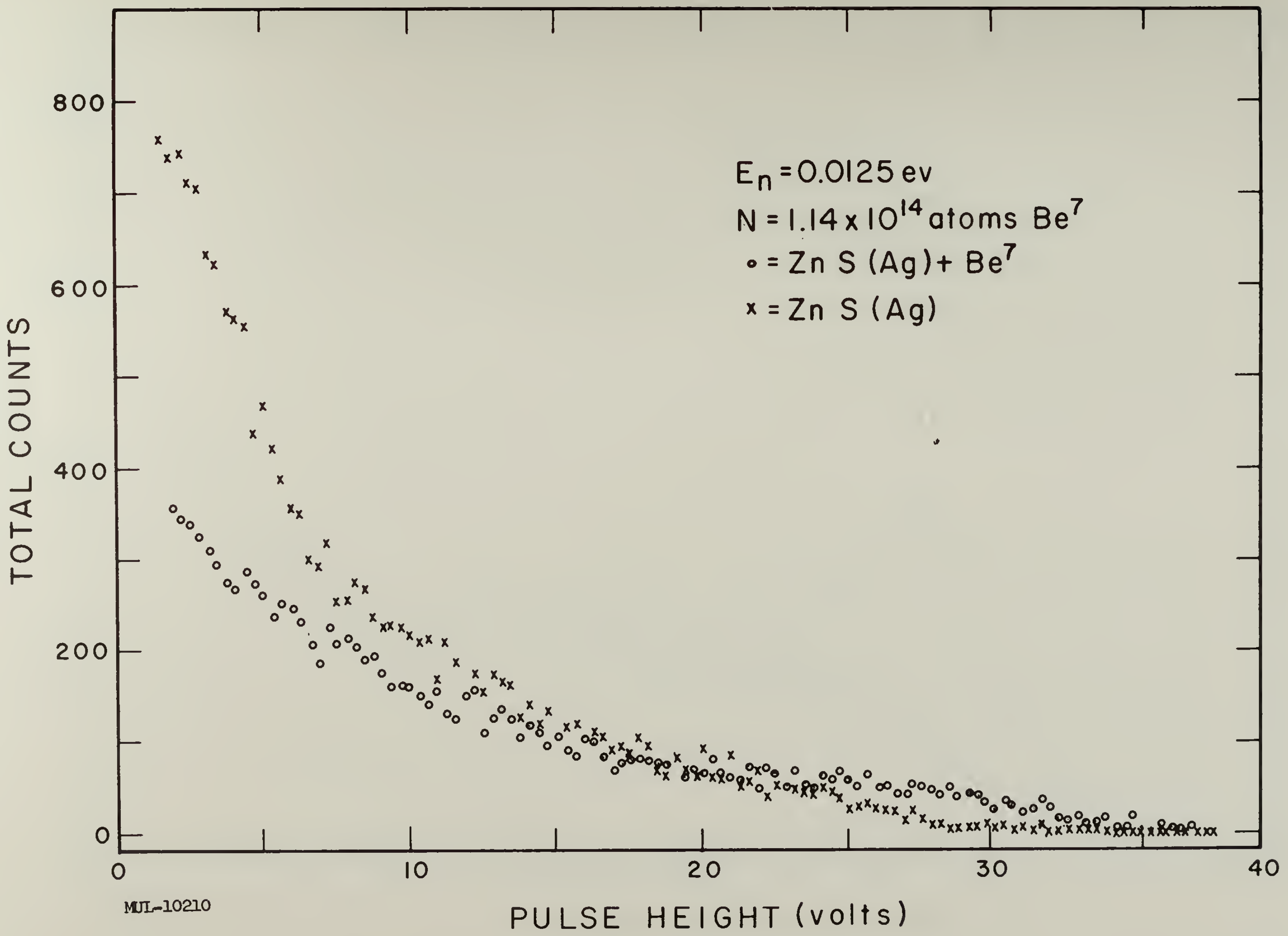

Fig. 6. ZnS(Ag) counter response.

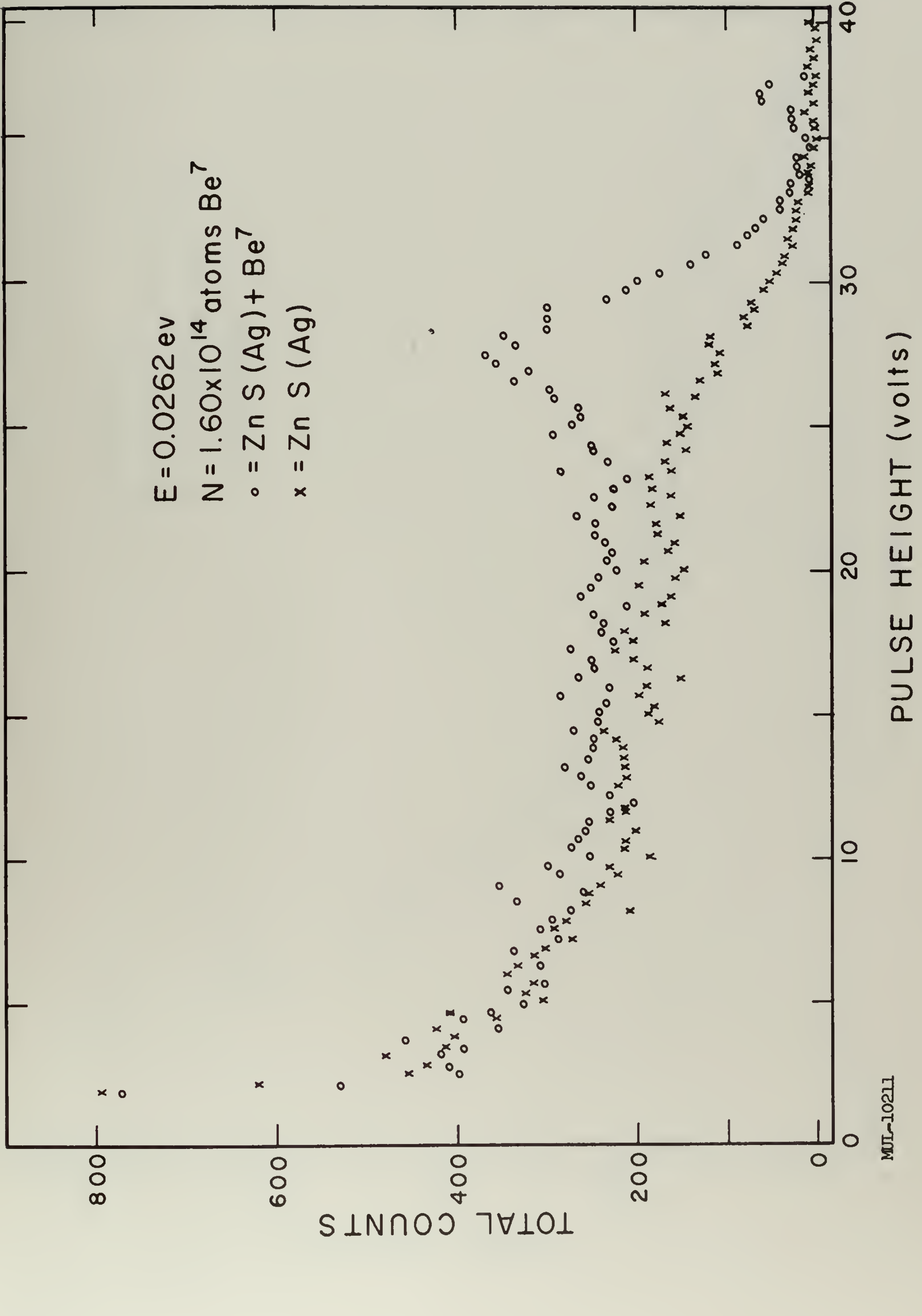

Fig. 7. ZnS(Ag) counter response.

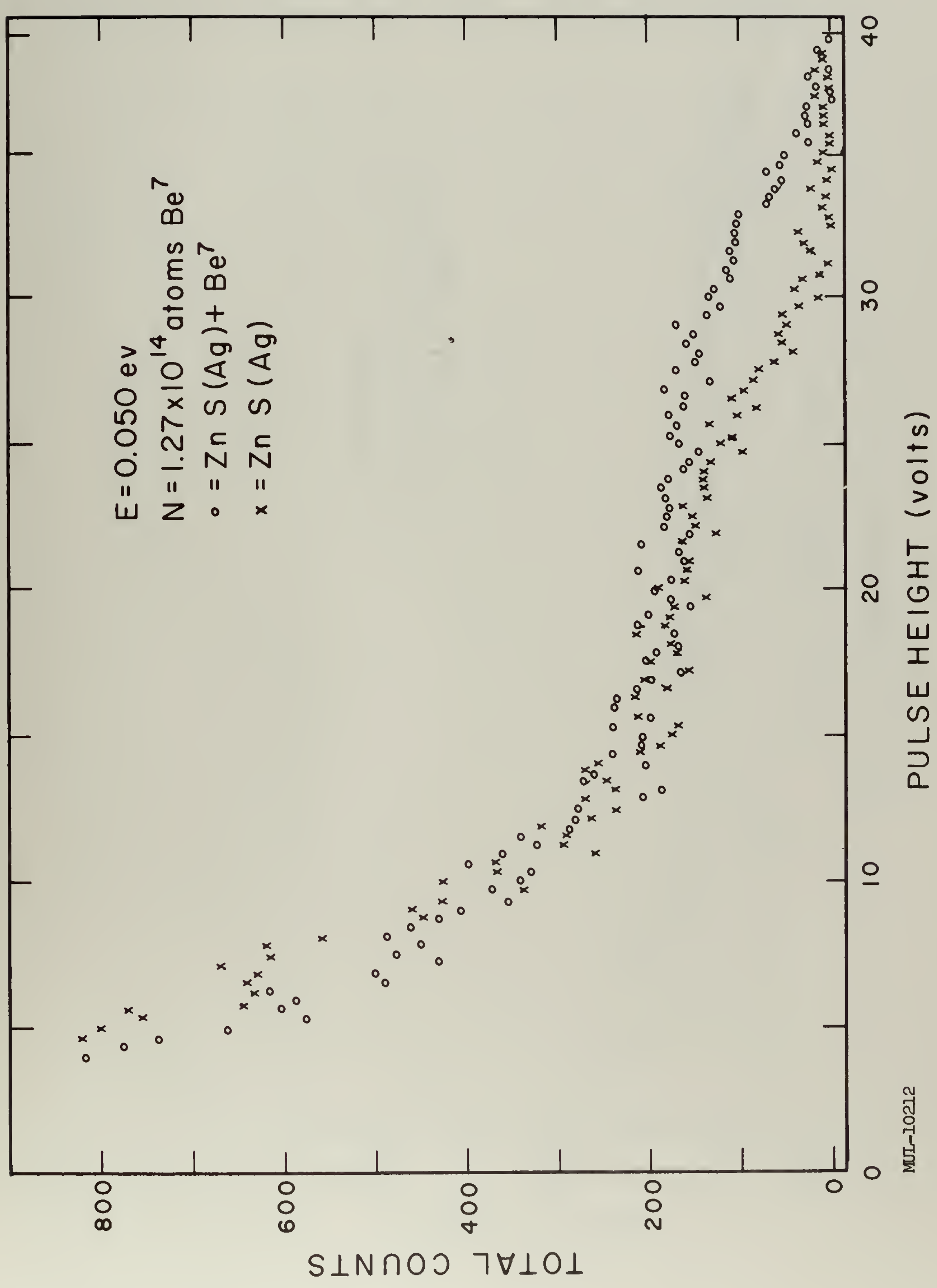

Fig. 8. ZnS(Ag) counter response.

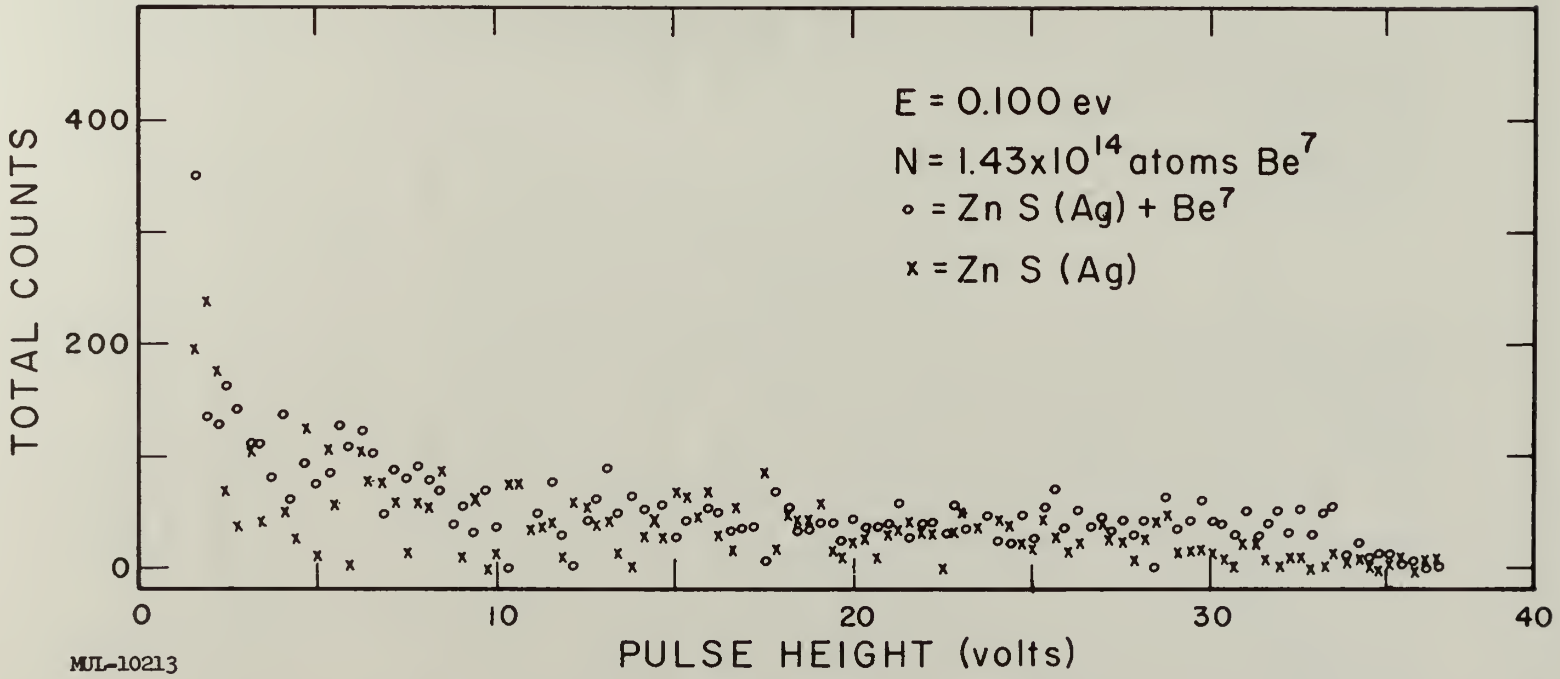

Fig. 9. ZnS(Ag) counter response.

reflection of the $Be^7(n,p)Li^7$ response to the neutron beam. The number of events recorded thus attributable to Be^7 response is listed in the following table.

Primary neutron energy (ev)	Apparent Be^7 events recorded (250 min)	BF_3 monitor response (c/cm^2 min)	Amount of Be^7 present (atoms)
0.0125	859	4.82×10^5	1.14×10^{14}
0.026	6794	6.91×10^5	1.60×10^{14}
0.050	3462	6.97×10^5	1.27×10^{14}
0.100	21	4.54×10^5	1.43×10^{14}

Comparison of the BF_3 monitor response with gold-foil activation readings indicates the monitor response to be about 20% efficient. It is noted that the latter two energy points are approximately the second-order energies for the first two energy points. Thus it may be seen that second-order response at 0.026 and 0.050 ev is probably quite small while at 0.0125 ev it may be quite large. This leads to the conclusion that there may be a large neutron activation cross section for Be^7 in the region of 0.026-0.050 ev in the form of a resonance. Such a resonance would help to explain the unusually large cross section for the $Be^7(n,p)Li^7$ reaction to thermal neutrons observed by Hanna. However, the main significance of these results is that the reaction can be observed by this method and more detailed measurements may now be accomplished.

VI. CONCLUSIONS

The problem has been to devise a method and equipment for the study of the neutron activation of Be^7 as a function of energy in the thermal region. This problem has been attacked in two parts: first, to produce a monoenergetic beam of neutrons of intensity sufficient to overcome the handicap of extremely small sample size, and second, to develop a

practical method of detecting the desired events. A neutron diffraction crystal spectrometer has been assembled of sufficient resolution and producing a sufficient intensity of monochromatic neutrons to insure reasonable statistics with the available sample size. It has been shown that the reaction can be observed with the use of ZnS(Ag) cyrstals in this spectrometer. Preliminary investigation shows that the cross section can be measured and indicates the possibility of a resonance existing in the thermal region.

Considerable work remains to be accomplished in accurately determining the harmonic contamination of the neutron bean and the resolution of the spectrometer. Improvement in detectors is also highly desirable to increase reliability, efficiency, and resolution for the study of this reaction.

VII. ACKNOWLEDGMENTS

The author is deeply indebted to Drs. Robert E. Donaldson and S. Warren Mead for many enlightening discussions, helpful comments, and suggestions offered in connection with this project, and to Mr. Donald J. Groves for his invaluable assistance during most of this project. Appreciation is also due the staff of the Livermore Pool Type Reactor Facility for their technical assistance and to Drs. A. J. Kirschbaum and J. Carothers for their interest and encouragement.

This work was done under the auspices of the U. S. Atomic Energy Commission.

VIII. REFERENCES

(Aj 59) F. Ajzenberg-Selove and T. Lauritzen, Nuclear Phys. **11**,35 (1959).

(Al 47) J. S. Allen, Rev. Sci. Instr. **18**,739 (1947).

(Ba 55a) G. E. Bacon, *Neutron Diffraction* (Oxford Press, 1955), pp. 61-73.

(Ba 55b) Ibid., p. 82.

(Do 59) R. E. Donaldson, private communication.

(Ha 59) R. Haas and F. J. Shore, Rev. Sci. Instr. **30**,17 (1959).

(Ha 55) R. C. Hanna, Phil. Mag. **46**,381 (1955).

(Id 59) G. M. Iddings, private communication.

(Ke 54) G. R. Keepin, Rev. Sci. Instr. **25**, 30 (1954).

(Ma 58) R. L. Macklin and J. H. Gibbons, Phys. Rev. **109**, 105 (1958).

(Ma 60) J. Mattingly, private communication and laboratory notes.

(Me 59) S. W. Mead, private communication.

(Mo 55) A. Moljk, R. W. P. Drever, and S. C. Curran, Rev. Sci. Instr. **26**, 1034 (1955).

(Sa 56) V. L. Sailor, H. L. Foote, Jr., H. H. Landon, and R. E. Wood, Rev. Sci. Instr. **27**, 26 (1956).

(Se 58) R. E. Segel, J. V. Kane, and D. H. Wilkinson, Phil. Mag. **3**, 204 (1958).

(Sz 59) P. Szabo, Nuclear Instr. and Meth. **5**, 184 (1959).

LEGAL NOTICE

This report was prepared as an account of Government sponsored work. Neither the United States, nor the Commission, nor any person acting on behalf of the Commission:

A. Makes any warranty or representation, expressed or implied, with respect to the accuracy, completeness, or usefulness of the information contained in this report, or that the use of any information, apparatus, method, or process disclosed in this report may not infringe privately owned rights; or

B. Assumes any liabilities with respect to the use of, or for damages resulting from the use of any information, apparatus, method or process disclosed in this report.

As used in the above, "person acting on behalf of the Commission" includes any employee or contractor of the commission, or employee of such contractor, to the extent that such employee or contractor of the Commission, or employee of such contractor prepares, disseminates, or provides access to, any information pursuant to his employment or contract with the Commission, or his employment with such contractor.

thesB795
A spectrometer for study of neutron acti
3 2768 002 07407 2
DUDLEY KNOX LIBRARY